# P1.52 AN EXAMINATION OF JUPITER'S GREAT RED SPOT AND OTHER VORTICES USING THE EPIC MODEL

Christopher J. Melick*[,1], Hisham Md. Anip[1], Andrew Kunz[1], Raul Morales-Juberías[2], Anthony R. Lupo[1], and Patrick S. Market[1]

[1]Department of Soil, Environmental, and Atmospheric Sciences
University of Missouri-Columbia
Columbia, MO

[2]Comparative Planetology Laboratory
University of Louisville
Louisville, KY

## 1. INTRODUCTION

A significant problem in the general study of the atmospheric characteristics of an extraterrestrial planet is that inferences must be made from remote sensing observations of limited areas. However, any data or observations are better than none, and from them one can understand the way the weather works on any planet, not just on Earth. In the case of Jupiter, one of the areas of fascination is with the Great Red Spot (GRS). The oldest known anticyclone of its kind, there have been numerous dynamical assessments of this spot, as well as other features on the rest of the planet (e.g., Bagenal et al. 2004). However, these assessments only examined Jupiter's fundamental meteorological characteristics but were not able to fully explain the various processes at work. This study furthers previous work by taking a look at a few of the basic mechanisms surrounding the GRS and other minor phenomena through the calculation of barotropic instability, various forcing terms in the omega equation, as well as other parameters. From this data, the present analysis should illuminate the dynamic and thermodynamic processes of Jupiter's atmosphere. For this purpose, we use simulation output fields generated from the Explicit Planetary Isentropic-Coordinate (EPIC) model (e.g., Dowling et al. 1998), developed at the University of Louisville.

**Corresponding author**: Christopher J. Melick, University of Missouri-Columbia, 370 McReynolds Hall, Columbia, MO 65211. E-mail: cjmzr5@mizzou.edu

## 2. DATA

For this study, the simulation data for Jupiter are obtained from the EPIC model (Dowling et al. 1998) with the help of Raul Morales-Juberias at the University of Louisville. While most numerical weather models are utilized explicitly to reproduce Earth's atmospheric dynamics and thermodynamics, the EPIC model is a general circulation model (GCM), which can be applied to atmospheric studies on several planets within the solar system. From the dataset provided, zonal and meridional wind components (u and v), temperature (T), and pressure (p) values were utilized in the analysis of the GRS. A simulation of this anticyclonic storm is available from the website location: http://solberg.snr.missouri.edu/People/melick/files/jupiter/simulation/STrD02.mov. In this study, a grid point spacing of approximately 0.2º latitude by 0.4º longitude was utilized for the following domain: 10.1º S - 34.9º S and 0.2º E - 99.8º E. The model architecture employs the hydrostatic primitive equations and an isentropic coordinate system, with the vertical resolution decreasing with increasing altitude. In particular, eight isentropic levels from 170 K to 1700 K were available for examination for a forecast period of 49 days. Upon analysis of this dataset, all figures for the resulting diagnostics were then displayed utilizing MATLAB software. For further specifics on the EPIC model, consult Dowling et al. (1998).

## 3. METHODOLOGY

### a) *Isentropic Method*

Large-scale vertical velocities are estimated to be approximately $10^{-3}$ $ms^{-1}$ on Jupiter (Bagenal et al. 2004), which is about an order of magnitude smaller than those typically experienced on Earth. Furthermore, the fact that these vertical motions are typically a few orders of magnitude smaller compared to their horizontal counterpart can lead one to conclude that large-scale updrafts and downdrafts are rather trivial and therefore could be neglected. In the case of our own planet, however, the presence of pure geostrophic flow is not sufficient to account for the vertical transport of atmospheric properties and the adiabatic temperature changes required to develop clouds and precipitation systems, the latter being a necessary and important constituent in the hydrologic cycle. Unfortunately, direct measurements of vertical motions are not possible due to their considerably small values, but rather must be estimated utilizing other known meteorological variables (Smith 1971). A common methodology for such calculations involves expanding the total derivative of pressure with respect to time in isentropic coordinates, otherwise known as the isentropic method (Market el al. 2000):

$$\omega_\theta = \frac{dp}{dt} = \left(\frac{\partial p}{\partial t}\right)_\theta + \vec{V}_h . \nabla_\theta P + \frac{\partial p}{\partial \theta}\frac{d\theta}{dt} \quad \textbf{(1)}$$

(A) (B) (C)

where the right hand side terms (A), (B) and (C) represent the local time tendency of pressure, pressure transport, and the change in potential temperature due to diabatic effects on an isentropic surface, respectively. A positive sign from any of the right-hand side terms corresponds to downward motion, whereas a negative response indicates upward motion. Thus, this means that ascent (descent) occurs in this framework as the isentropic surface moves upward (downward) to lower (higher) pressure (term A), as air parcels translate along an isentropic surface from higher (lower) to lower (higher) pressure (term B), and/or as diabatic heating (cooling) occurs in the local atmosphere. While estimates of $\omega_\theta$ from each contribution would be desirable, the authors are unaware of any relevant parameterization which might be applicable for the latter forcing mechanism. Thus, the total vertical motion response is calculated from only the first two adiabatic components.

### b) *Barotropic Instability*

$$\frac{\partial f}{\partial y} - \frac{\partial^2 u}{\partial^2 y} \quad \textbf{(2)}$$

The above condition describes the tendency for a wave perturbation to amplify horizontally, where the first term represents meridional changes in planetary rotation (beta) and the second represents meridional changes in the relative vorticity (Haltiner and Williams 1980). Oftentimes, the beta term tends to dominate within a jetlike current, and therefore, produce a barotropically stable atmosphere. As a result, the speed of the background flow will increase as kinetic energy is drawn away from any small scale disturbances. The reverse scenario, however, is possible if the gradient of the absolute vorticity changes sign at some point over the specified domain. In particular, Haltiner and Williams (1980) state that a disturbance will grow if and only if the wave tilts opposite to the shear, a situation that occurs when the following barotropic instability criterion is met: $\frac{\partial^2 u}{\partial^2 y}_{MAX} > \frac{\partial f}{\partial y}$. Thus, while positive values for (2) indicate a stable atmosphere with respect to horizontal shear, barotropic instability corresponds to negative values for the above expression.

*c.) Omega Equation Forcing Terms*

Absolute vorticity advection is posed as:

$$-\vec{V}_h.\nabla_h\zeta_a \quad \textbf{(3)}$$

while temperature advection is :

$$-\vec{V}_h.\nabla_h T\,. \quad \textbf{(4)}$$

In the above expressions, $\vec{V}_h$ is the horizontal wind vector with components (u,v), $T$ the temperature, and $\zeta_a$ is the absolute vorticity vector ( $\zeta_a = \zeta + f$ ). The conventional form of the omega equation is appealing because it provides a practical means to qualitatively diagnose the vertical motion (ω) field utilizing basic meteorological processes. In particular, the determination of areas of ascending and descending motion can be determined simply by knowing the sign of the right-hand-side terms. Since horizontal and vertical fields of ω typically exhibit a sinusoidal shape, Holton (2004) asserts that positive (negative) values for forcing mechanisms will produce upward (downward) motion. Previous studies by Krishnamurti (1968b), Räisänen (1995), and others have shown that (3) and (4) are the most significant factors in producing synoptic-scale vertical motions. Thus, this means that ascent (descent) will usually occur in regions where absolute vorticity advection increases (decreases) with height and warm (cold) air advection are present (Walters 2001).

*d.) Finite Differencing*

In order to calculate horizontal derivatives, second-order and fourth-order finite differencing was utilized for grid points within the interior of the domain. Similarly, second-order finite differencing was utilized for vertical derivatives, not including the lowest and highest isentropic surface. Furthermore, centered finite differencing with a temporal resolution of 24 hours was also applied in the case of tendency quantities.

## 4. RESULTS

Recent attempts to reproduce the merger of Jupiter's White Ovals utilizing the Explicit Planetary Isentropic-Coordinate (EPIC) atmospheric model have been relatively successful (Morales-Juberías et al. 2003). Still, the physical processes responsible for these atmospheric features have not been sufficiently explained. While relatively good agreement with observations is essential to determining the performance of the model and thus its usefulness, the present study goes a step further into better understanding the behavior of Jupiter's atmosphere. In order to assess the dynamics, however, a general synopsis of the weather pattern depicted by EPIC is preferred initially. For this purpose, pressure and temperature fields for three lower isentropic levels are shown in figs. 1 and 2, respectively, with the model simulations verifying at 360 hours (15 days), 720 hours (30 days), and 1080 hours (45 days). Furthermore, an illustration of the wind flow regime is also depicted for the 170 K potential temperature surface during this same time period (Figs. 3,4,5). These analyses show a large, warm-core high pressure system with counter-clockwise rotation propagating from east to west over a considerable portion of the domain. As this occurs, smaller vortices are occasionally interacting with the much larger Great Red Spot (GRS). The poleward side westerly jet and equatorward side easterly jet streams imply the presence of anticyclonic shear from about 15° to 30° south, which was similarly noted by Bagenal et al. (2004). Above this lower-level configuration, the GRS thermal/pressure pattern switches to more of a colder-core, low pressure system. While the cohesive nature of the disturbance becomes less distinct with increasing altitude, temporal variations appear to be comparatively less significant. For instance, intensification of the high pressure system was minimal for the model simulation, as revealed by Fig. 1 and further confirmed by near zero central pressure tendency values (not shown).

Adiabatic vertical motions, calculated from (1), are shown in Figs. 6, 7, and 8 for each of the three forecast times. As air parcels approach the anticyclone from either the southern or northern side, isentropic descent occurs as the flow progresses from lower to higher pressure. Alternatively, isentropic ascent occurs immediately downstream from the system as the pressure of the air stream decreases. This four quadrant pattern is prevalent over the lower half of the vertical profile and the physical interpretation gives the impression that a significant portion of $\omega$ arises from the pressure transport term (B). Often times, meteorologists only consider this mechanism as an accurate estimate of the vertical motion field. However, Market et al. (2000) has shown that this does not always hold true and may give a substantial underestimate of the correct value. Thus, in order to eliminate any uncertainty on the matter, percentage contributions to the total response are calculated for the two individual adiabatic components and presented as averages over the time period in Table 1. While the pressure tendency term (A) is the predominant factor in producing vertical velocities at the highest potential temperature surface, ascent and descent along an isentropic surface accounts for at least half of the magnitude of omega through a greater depth of the Jovian atmosphere, with a significant contribution (over 70 percent) in the lowest portion. Finally, mean absolute values for adiabatic vertical velocities, also presented in Table 1, indicate that typical magnitudes are on the order of 0.1 $\mu$b $s^{-1}$ at the lower altitudes and decrease rather markedly upon reaching the upper atmosphere.

Previous work in synoptic meteorology utilizing the omega equation (numerical method) has shown that vorticity (3) and temperature advections (4) are the primary forcing mechanisms for producing synoptic-scale vertical motions (e.g. Krishnamurti 1968b; Räisänen 1995). This approach is utilized for Jupiter's atmosphere in order to ascertain the most significant factors affecting omega as well as provide an independent means of checking the results computed from (1). In order to correctly determine spatial means, however, the size of the domain needed to be restricted so as to avoid cancellation between values of opposite sign. Since all three forecast times exhibited only minor variations in the $\omega$ fields, the analysis of the EPIC model output is further limited to only the first verification time (day 15). Thus, vorticity and temperature advections are calculated for a 7 x 7 grid point region centered on the location experiencing the strongest ascent at the 170 K potential temperature surface (Fig. 6). Results for these two terms along with the vertical motions are expressed as averages for each isentropic level in Table 2. Since upward (downward) motions generally occur in regions where vorticity advection increases (decreases) with height and where warm (cold) air advection are present (Walters 2001), the response produced throughout most of the vertical profile is in agreement with what would be expected from theory.

Other than the strong temperature advections associated with the anticyclone (Table 2), thermal gradients at each isentropic level appear to be relatively small (Fig. 2). While this might suggest that Jupiter's atmosphere should have a robust barotropic component, computations of vertical wind shear were also considered in this study to further provide evidence for this hypothesis. Mean absolute values for the latter are displayed in Table 3 at one upper-level isentropic surface and one lower-level isentropic surface for the first verification time (day 15). Results indicate that the meridional and zonal wind shear components are comparable in magnitude, with both exhibiting a significant increase upon reaching the upper atmosphere. Furthermore, these estimates are similar compared to typical conditions which exist in the Earth's troposphere. Predominantly, the airstream pattern for Jupiter is more disorganized at higher altitudes due to the greater number of smaller vortices present (e.g., compare fig. 6a to fig. 6h). Thus, the winds speeds are not only stronger aloft, but the direction of the flow is more variable compared to much lower levels, where the background zonal component is prevalent. Since significant vertical shear exists in spite of minimal horizontal temperature advections, this scenario suggests that Jupiter's atmosphere might be classified as equivalent barotropic (Wallace and Hobbs 1977). Consequently, any instability present would be most likely associated with amplification of horizontally oriented disturbances. In order to investigate this hypothesis further, calculations of barotropic instability (2) are performed for one time period utilizing EPIC model output (not shown). Since results produced positive values over the entire domain, this diagnostic implies that the $\beta$ term is relatively more important than gradients of relative vorticity. Consequently, this would suggest that embedded short-waves will have a tendency to damp and lose energy barotropically to the mean Jovian atmospheric flow (e.g. Haltiner and Williams 1980). Furthermore, inspection of the numerical simulation presented in this study appears to favor this assertion, especially considering the fact that most of the smaller vortices in the domain eventually merged with the much larger GRS.

## 5. SUMMARY

The Great Red Spot (GRS) on Jupiter is a great anti-cyclonic storm akin to a blocking high on Earth, but it is enormous (semi-major axis > 22,000 km) and it has been continuously observed for at least 120 years. Historically, several studies have been conducted by researchers in order to understand its nature. Unfortunately, some physical processes related to it have not been entirely explained yet. In order to better understand the most important physical processes affecting Jupiter's atmosphere, a few sample diagnostics are presented utilizing EPIC model simulations. The synopsis of a westward propagating, warm-core high pressure center (i.e., GRS) in the Jovian southern hemisphere reveals that storm systems have a relatively shallow vertical circulation pattern, with changes in intensity being relatively minimal. As air parcels approach the anticyclone from either the northern or southern side, isentropic descent occurs as the flow progresses from lower to higher pressure. Alternatively, isentropic ascent occurs immediately downstream from the system as the pressure of the air stream decreases. While the pressure tendency term (A) is an important factor in producing vertical velocities for the upper isentropic surfaces, a statistical analysis confirmed that the pressure transport term (B) accounted for more than 70 percent of the magnitude of $\omega$ through a greater depth of the atmosphere. Typical values for large-scale vertical motions were found to be on the order of 0.1 $\mu$b $s^{-1}$ at the lower altitudes, with a noticeable decrease in magnitude upon reaching the upper atmosphere.

Consultation of the omega equation provided a means to check the results obtained from the isentropic method. A qualitative comparison reveals that both approaches were generally consistent in the type of vertical motion produced, with a combination of both the temperature and vorticity advections determined to be contributing forcing mechanisms. Still, analyses of more regions in the domain are required in order to increase the sample size, thereby obtaining more thorough results. While other physical processes, such as latent heat release, could be significant in forcing ascent and descent, this particular mechanism was not addressed mainly because of no known scheme to formulate a mathematical representation for the planet. Given that the flow was predominately two dimensional and thermal advections were generally small in magnitude, relatively strong vertical wind shear values, similar to those found on Earth, gave the impression that Jupiter's atmosphere might have a significant equivalent barotropic component. The corresponding instability results showed that the criterion for horizontal accelerations was never met at any point over the entire domain, with gradients in absolute vorticity of positive sign everywhere. Thus, kinetic energy has a tendency to cascade from smaller to larger scales in barotropically stable conditions as wavelike disturbances weaken with time. For future work, it would be interesting to investigate whether or not convective overturning might occur by analyzing several stability indices, such as potential instability.

## REFERENCES

Bagenal F., T.E. Dowling, and W.B. Mckinnon, 2004: *Jupiter: The Planet, Satellites, and Magnetosphere.* Cambridge University Press. 700pp.

Dowling, T.E., and Coauthors, 1998: The Explicit Planetary Isentropic-Coordinate (EPIC) atmospheric model. *Icarus,* **132,** 221-238.

Haltiner G.J., and R.T. Williams, 1980: *Numerical Prediction and Dynamic Meteorology: Second Edition*. John Wiley & Sons, 477pp.

Holton, J.R., 2004: *An Introduction to Dynamic Meteorology.* 4th ed. Elsevier Academic Press, 529pp.

Krishnamurti, T.N., 1968b: A study of a developing wave cyclone. *Mon Wea Rev.,* **96**, 208-217.

Market, P.S., J.T. Moore, and S.M. Rochette, 2000: On calculating vertical motions in isentropic coordinates. *Nat. Wea. Dig.*, **24**, 31-37.

Morales-Juberías, R., A. Sánchez-Lavega, and T.E. Dowling, 2003: EPIC simulations of the merger of Jupiter's White Ovals BE and FA: altitude-dependent behavior. *Icarus,* **166,** 63-74.

Räisänen J., 1995: Factors affecting synoptic-scale vertical motions: a statistical study using a generalized omega equation. *Mon. Wea. Rev.*, **123**, 2447-2460.

Smith, P.J., 1971: An analysis of kinematic vertical motions. *Mon. Wea. Rev.,* **99**, 715-724.

Wallace, J.M., and P.V. Hobbs, 1977: *Atmospheric Science: An Introductory Survey*. Academic Press, 467 pp.

Walters, M.K., 2001: A simple example of Galilean invariance in the omega equation. *Bull. Amer. Meteor. Soc.,* **82**, 463-472.

Table 1. Percentage contributions to the adiabatic vertical motions from the pressure tendency term and pressure transport term, with values given for each isentropic level in the EPIC model. Mean absolute values for the total $\omega$ ($\mu$b $s^{-1}$) are also presented in the last column. All results are expressed as averages over the three verification time periods of the model (day 15, day 30, and day 45).

| Isentropic Level | Tendency Term | Transport Term | Total $\omega$ ($\mu$b $s^{-1}$) |
|---|---|---|---|
| 170 K | 26 % | 74 % | $1.2 * 10^{-1}$ |
| 180 K | 20 % | 80 % | $4 * 10^{-2}$ |
| 190 K | 28 % | 72 % | $4 * 10^{-3}$ |
| 230 K | 30 % | 70 % | $9 * 10^{-4}$ |
| 350 K | 48 % | 52 % | $2 * 10^{-4}$ |
| 590 K | 56 % | 44 % | $5 * 10^{-5}$ |
| 1000 K | 50 % | 50 % | $2 * 10^{-5}$ |
| 1700 K | 97 % | 3 % | $2 * 10^{-6}$ |

Table 2. Vorticity advection ($s^{-2}$) and temperature advection (K/s) over a small region (7 x 7 grid point domain) encompassing the strongest ascent at the 170 K isentropic surface. Adiabatic vertical motions ($\mu$b $s^{-1}$) over the same area are presented as well. Results are limited to the first verification time period (day 15) and expressed as averages for each isentropic level above the event.

| Isentropic Level | Vorticity Advection | Temperature Advection | Total $\omega$ ($\mu$b $s^{-1}$) |
|---|---|---|---|
| 170 K | $-2 * 10^{-10}$ | $3 * 10^{-3}$ | -4.6 |
| 180 K | $8 * 10^{-10}$ | $2 * 10^{-3}$ | -1.3 |
| 190 K | $1 * 10^{-9}$ | $-7 * 10^{-5}$ | $-2 * 10^{-2}$ |
| 230 K | $1 * 10^{-9}$ | $-5 * 10^{-4}$ | $2 * 10^{-2}$ |
| 350 K | $3 * 10^{-10}$ | $-1 * 10^{-4}$ | $8 * 10^{-4}$ |
| 590 K | $9 * 10^{-11}$ | 0 | $-1 * 10^{-4}$ |
| 1000 K | $3 * 10^{-11}$ | 0 | $1 * 10^{-5}$ |
| 1700 K | $-4 * 10^{-13}$ | 0 | $2 * 10^{-6}$ |

Table 3. Mean absolute values for vertical wind shear (m $s^{-1}$ $Pa^{-1}$) at a lower-level and upper-level isentropic level, with results limited to the first verification time period (day 15).

| Isentropic Level | $\frac{\partial U}{\partial P}$ (Zonal Component) | $\frac{\partial V}{\partial P}$ (Meridional Component) |
|---|---|---|
| 180 K | $8.85 * 10^{-6}$ | $2.72 * 10^{-6}$ |
| 1000 K | $2.16 * 10^{-3}$ | $1.99 * 10^{-3}$ |

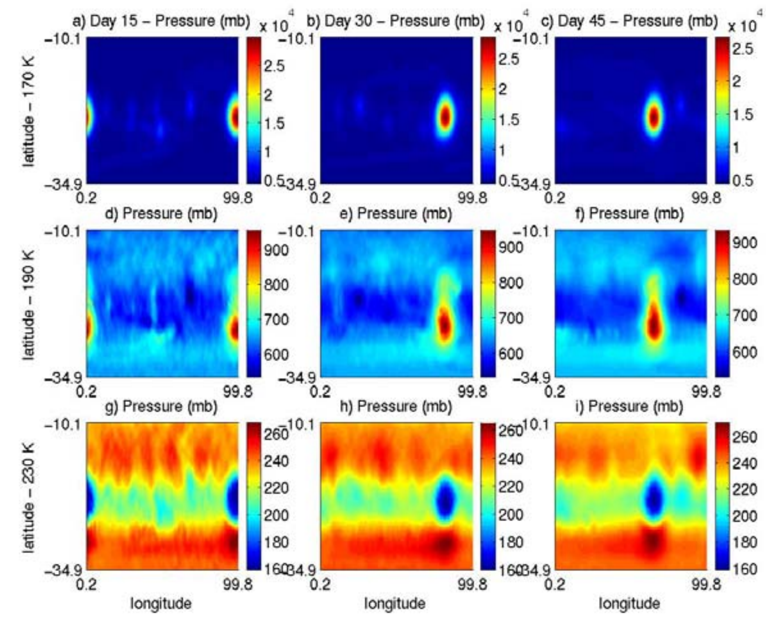


Fig. 1) EPIC model simulation of Jupiter's atmosphere (0.2 E – 99.8 E; 34.9 S - 10.1 S). Pressure (mb) is displayed for the 170 K isentropic level at forecast a) day 15, b) day 30, and c) day 45. Similar plots are also shown for the 190 K [ d), e), f) ] and 230 K [ g), h), i) ] isentropic levels.

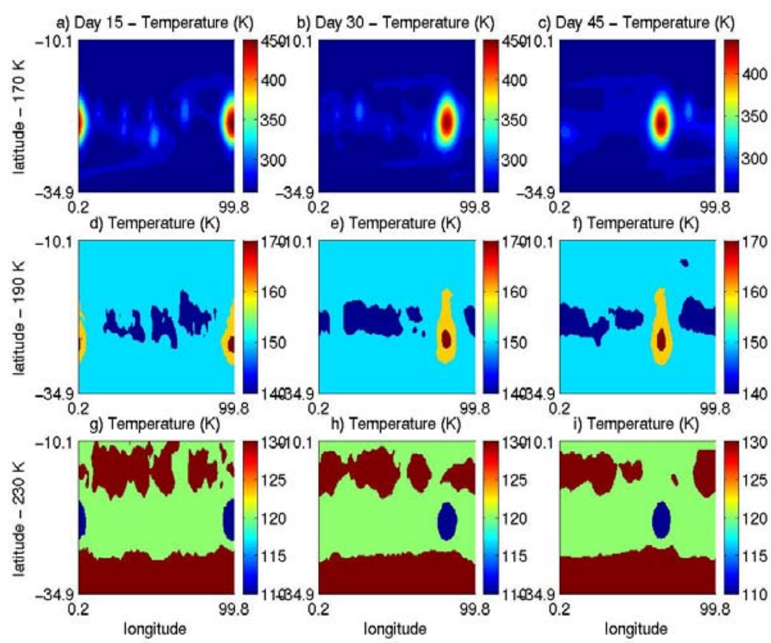


Fig. 2. As in Fig. 1 except for temperature (K).

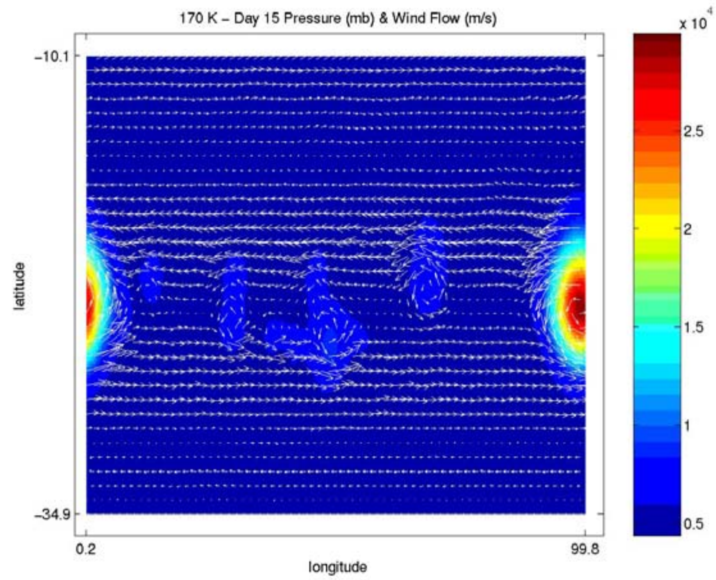


Fig. 3. 170 K isentropic surface pressure (mb) and wind flow (m/s) at forecast day 15 in EPIC model simulation.

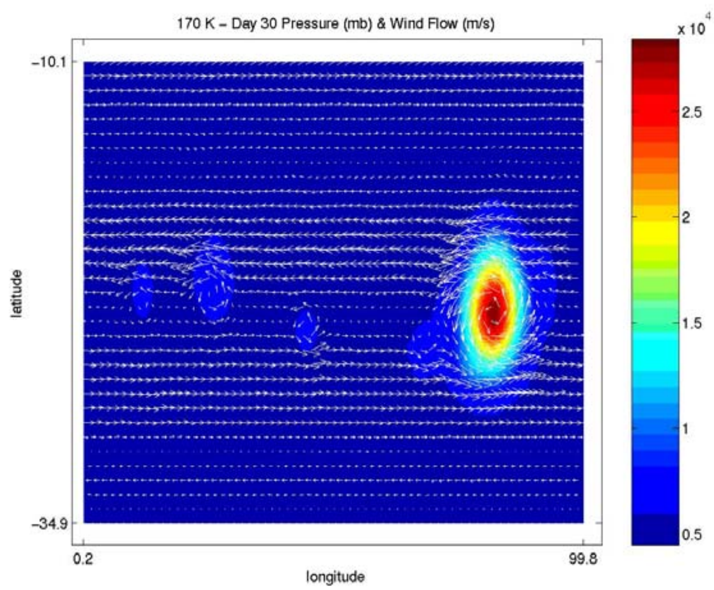


Fig. 4. As in Fig. 3 except for forecast day 30.

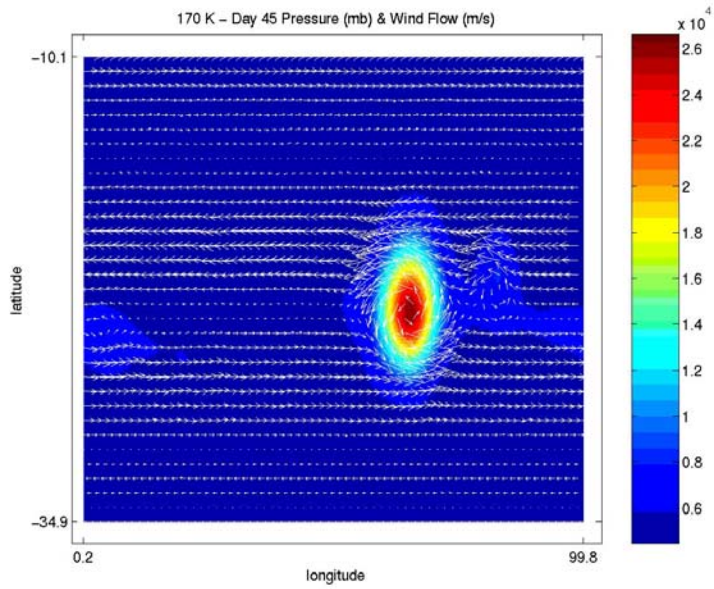


Fig. 5. As in Fig. 3 except for forecast day 45.

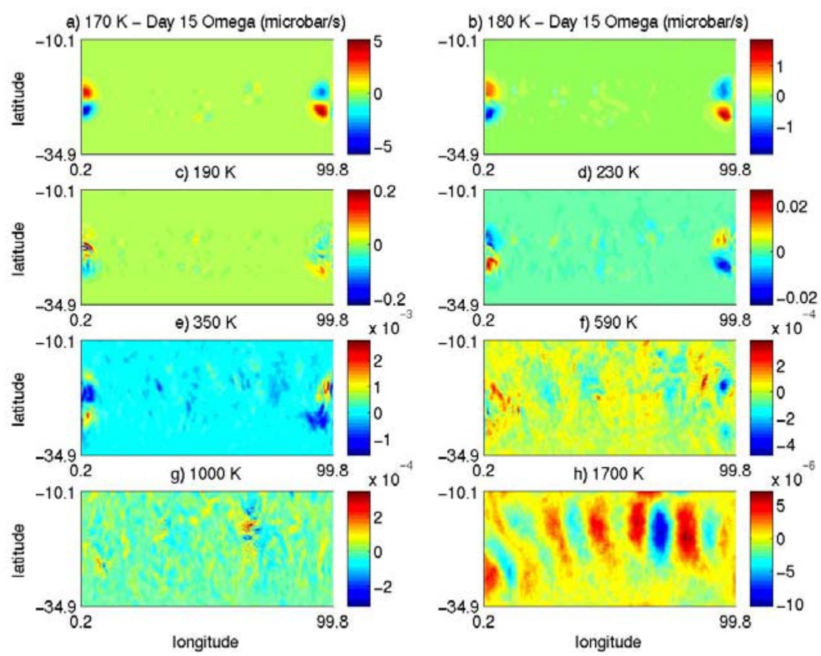


Fig. 6. Adiabatic vertical motions ($\mu b\ s^{-1}$) computed from the isentropic method for eight isentropic levels for forecast day 15 in EPIC model simulation.

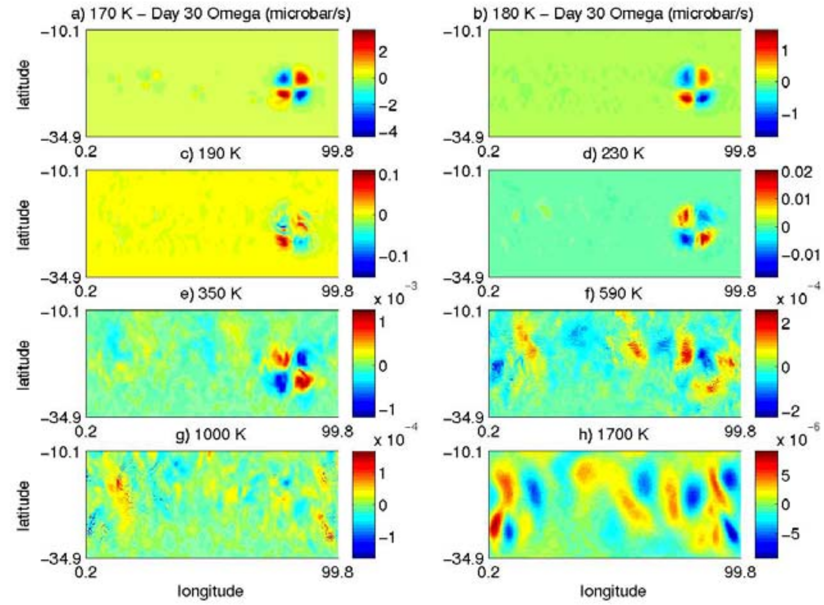


Fig. 7. As in Fig. 6 except for forecast day 30.

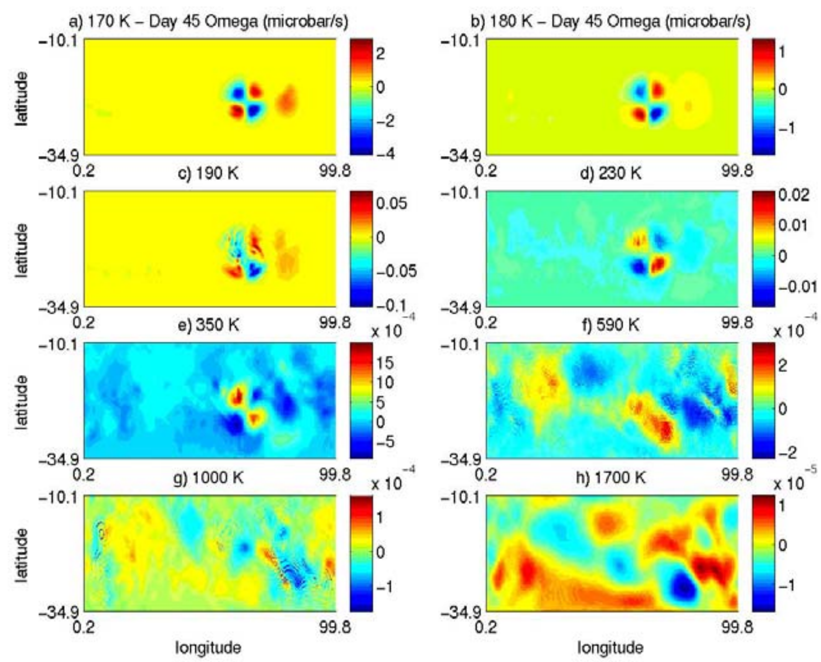


Fig. 8. As in Fig. 6 except for forecast day 45.